Energy Analysis of a Hall Thruster Cluster

Brian E. Beal and Alec D. Gallimore
Plasmadynamics and Electric Propulsion Laboratory
Department of Aerospace Engineering
The University of Michigan
Ann Arbor, MI 48109

ABSTRACT

In an effort to understand the technical issues related to using a cluster of Hall effect thrusters to accomplish missions requiring very high-power electric propulsion systems, testing of four Busek BHT-200-X3 thrusters has begun at both the Air Force Research Laboratory and the University of Michigan. Two separate instruments, the parallel-plate electrostatic energy analyzer and the retarding potential analyzer, have been used to measure the ion energy spectrum at various locations downstream of the low-power Hall thruster cluster. These results, when compared to measurements taken in the plume of a single thruster, indicate that clustering causes dramatic changes in the ion energy profiles. In particular, operating multiple thrusters seems to cause an increase in the fraction of ions at energies below the primary peak in the distribution. The large population of low energy ions is believed to be caused primarily by scattering due to elastic collisions between ions and neutral xenon atoms. Additionally, changes in the plasma potential profiles as a result of clustering may cause low energy ions to be preferentially deflected at small angles with respect to the cluster centerline. This mechanism is proposed as an explanation for several features of the presented ion energy spectra.

Introduction

Future Air Force plans foresee a need for electric propulsion systems capable of operating in the 100-150 kW power regime for use on orbit transfer vehicles and rescue vehicles capable of repositioning satellites that have exhausted their propellant load or failed to meet their operational orbit.[1,2] The most viable type of electric propulsion device for this class of mission is the Hall thruster due to its low specific mass, high thrust density, and high reliability. One method for reaching such high power levels involves clustering multiple moderately powered thrusters together to reach the total throughput desired.

A cluster of thrusters may have a slightly lower efficiency and higher dry mass than a single, similarly powered thruster since larger thrusters have historically performed better than smaller thrusters. A cluster, however, has several advantages over a monolithic thruster, including improved system reliability due to the inherent redundancy of running multiple engines and the ability to throttle the system by simply turning off one or more of the thrusters. Throttling the system in this way allows the cluster to operate at lower power without running any of the individual thrusters at off-design conditions. This aspect of a cluster may prove beneficial, for example, on a geosynchronous satellite where a high-power Hall thruster cluster could be used for the initial LEO-GEO transfer and one element of the cluster could then be used for north-south station keeping (NSSK). An additional, and perhaps very important, advantage of clustering is the high degree of system scalability. In principle, once the technical issues involved with operating a cluster are fully understood, a single flight-qualified engine could support a wide range of missions requiring various power levels by simply clustering the appropriate number of thrusters. Thus, enhanced scalability and flexibility make clusters attractive for many missions.

Although using a cluster of commercially available thrusters for primary propulsion appears to be advantageous for some missions, there are several systems integration issues that must be addressed before clusters can be used in flight.[1,2] Perhaps the most pressing issue is the need to understand the interaction of the plasma plumes with each other and with the spacecraft. In particular, it is imperative that the energy spectrum of a cluster plume be understood such that the effect of the plume on the lifetime of various spacecraft components can be predicted. In an effort to address this issue, the ion energy distribution downstream of a low-power Hall thruster cluster was studied using both a parallel-plate electrostatic analyzer (ESA) and a retarding potential analyzer (RPA). The results are compared to those obtained for a single thruster unit.

Experimental Setup

Cluster

The cluster used in these experiments was composed of four Busek BHT-200-X3 200-watt class Hall thrusters. An earlier version of this thruster was reported to operate at an anode efficiency of 42% and a specific impulse of 1300 seconds while providing 12.4 mN of thrust at the nominal operating conditions.[3] Each thruster has a mean diameter of 21 mm. The thrusters are arranged in a 2x2 grid with approximately 11.4 centimeters between the centerlines of adjacent thrusters. Each thruster is paired with its own Busek 3.2 mm diameter hollow cathode whose voltage is allowed to float independently of the others. Throughout these experiments, each thruster was operated at nominal conditions of 250 volts and 0.80 amps on anode and cathode xenon mass flow rates of 8.5 and 1.0 sccm, respectively. Figure 1 shows the cluster spacing and naming convention while Figure 2 is a view of the cluster during operation.

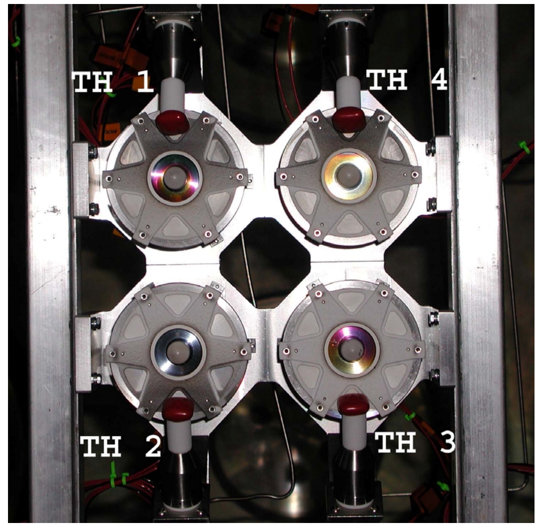

Figure 1: A cluster of four 200-watt Hall thrusters.

Figure 2: The cluster during operation.

Vacuum Chamber

The measurements described in this paper were conducted in the Large Vacuum Test Facility (LVTF) at the University of Michigan's Plasmadynamics and Electric Propulsion Laboratory (PEPL). The LVTF is a 6x9 meter, cylindrical, stainless steel clad vacuum chamber that is evacuated by seven CVI model TM-1200 cryopumps. The cryopumps provide a pumping speed of 500,000 liters per second on air and 240,000 liters per second on xenon for typical base pressures of approximately 2.5x10^{-7} Torr. For these experiments, only four cryopumps were used resulting in chamber pressures of 1.1x10^{-6} and 3.6x10^{-6} Torr corrected for xenon during single- and four-thruster operation, respectively.

Electrostatic Energy Analyzer

A 45°, parallel-plate type electrostatic energy analyzer consists of two parallel plates separated by a distance, d. One of the plates is electrically grounded while the other is biased to a positive potential, V_R, to reflect ions admitted through a slit of width w in the grounded baseplate. After being deflected by the applied electric field, E, ions of a selected initial velocity to charge ratio, u_i/q_i, pass through a second slit a distance L from the first slit and are collected by a detector as illustrated in Figure 3. Since only ions of a specific energy to charge ratio are collected, the ESA acts as a velocity per charge filter for a given ion species. For the specific case of a 45° ion injection angle, the properties of the collected ions are related to the voltage of the repelling plate by Equation 1, where m_i is the ion mass and q_i represents the ion charge. Defining the ion kinetic energy per charge as the equivalent ion voltage, V_i, allows the relationship to be written as Equation 2, where K_{45} is the spectrometer constant given by L/2d. Thus, the collector current measured as a function of the applied plate voltage is proportional to the ion energy per charge distribution. Note that this result is independent of the ion mass.

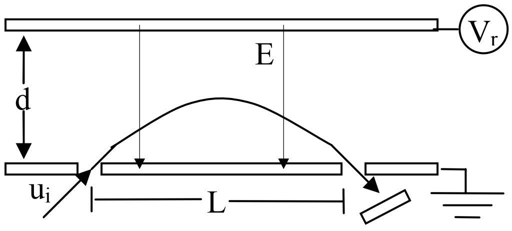

Figure 3: Simplified schematic of a 45° parallel-plate energy analyzer.

$$\frac{m_i u_i^2}{2q_i} = \left(\frac{L}{2d}\right) V_R \qquad (1)$$

$$V_i = K_{45} V_R \qquad (2)$$

Several ESAs of varying sizes have been used to study electric propulsion devices both at PEPL and elsewhere.[4-9] The instrument used for these measurements is very similar in size to one used successfully by Pollard to study a Hall thruster plume.[9] The main body of the ESA consists of a cube constructed of mica dielectric and measuring approximately 300 mm (12”) in each dimension. A dielectric material was chosen to reduce the disturbance to the plasma plume compared to that caused by the more common grounded devices. The inner surfaces of the box are coated with grounded aluminum foil to prevent charge accumulation within the instrument. Vent slots have been machined into the mica box to prevent an elevated pressure from occurring inside the device. Grounded aluminum baffles prevent ions from entering through the vent holes while allowing neutral atoms to escape.

The parallel plates are constructed of 1.5875 mm (0.0625”) thick aluminum and are separated by a distance, d, of 76.2 mm (3.0”). The rectangular slits in the base plate measure 1.5 x 15 mm (0.06” x 0.6”) and are 152.4 mm (6.0”) apart. Two field correction plates are placed between the main plates at one inch intervals and biased by resistor strings to reduce the adverse effects of fringing electric fields.

During data collection, the repelling plate voltage, V_R, was swept from 0 to 600 volts using a Keithley 2410 sourcemeter. The ion current collected at the detector was measured using a Keithley model 486 picoammeter. Both the plate voltage and the collected current were recorded using a PC running Labview software. Multiple ESA traces were recorded at each data point to verify the repeatability of the collected data. Figure 4 shows two sets of data collected 5°

off centerline for a single thruster. Note the very good repeatability of the traces, particularly at ion energies above 100 volts.

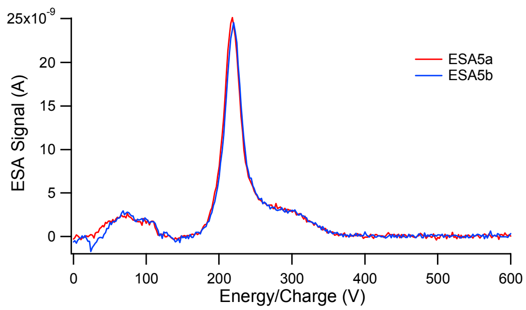

Figure 4: Sample ESA traces demonstrating the repeatability of the data.

<u>Retarding Potential Analyzer</u>

The retarding potential analyzer (RPA) diagnostic allows the collection of selectively filtered ions by applying a retarding potential across an inlet grid. For a given grid potential, only ions with energy to charge ratios (E/q) greater than the grid voltage pass through the inlet and reach the collector. The magnitude of the derivative of the resulting current-voltage characteristic, dI/dV, is then proportional to the ion energy distribution. The RPA used in these experiments was based on the multi-gridded energy analyzer design of Hutchinson.[10] It is composed of three grids and is shown schematically in Figure 5.

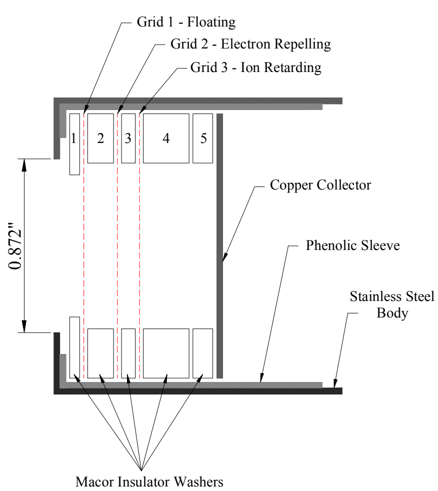

Figure 5: RPA schematic.

The outer body of the RPA is constructed of 316 stainless steel (SS) tubing, which was held at ground potential. A phenolic sleeve placed inside the body provides electrical isolation of the grids. All grids are identical and are cut from 316 SS, photochemically machined sheet with a thickness of 0.127 mm (0.005”). The grid openings are 0.2794 mm (0.011”) in diameter with a total open area fraction of 38%. Grid spacing is accomplished using Macor washers machined to provide correct separation. The collector is a simple copper disc. Electrical connections are accomplished by spot welding stainless steel wire to each grid. The wires are then routed along the inner edge of the phenolic sleeve and out the rear of the body. The washers and grids are sandwiched together by a spring placed behind the collector and held in place by a rear cover. Relevant spacing is summarized in Table 1.

Washer	Thickness	I.D.
1	1.067 mm	18.54 mm
2	3.353 mm	21.54 mm
3	1.727 mm	21.54 mm
4	6.553 mm	21.16 mm
5	6.553 mm	21.23 mm

Table 1: RPA washer thicknesses and inner diameters.

During operation, grid 1 was floated to provide a non-perturbing interface between the probe and the plasma while a Kikisui power supply was used to bias grid 2 30 V below ground to repel electrons. Grid 3 was swept from 0 to 600 V relative to ground using the Keithley sourcemeter. The resulting current to the collector was measured using the same picoammeter and Labview software discussed previously. A sample RPA current-voltage trace, a cubic spline fit to the data, and the corresponding ion energy distribution function are shown in Figure 6. These data were taken 0.5 m downstream of the thruster exit plane, 5º off centerline.

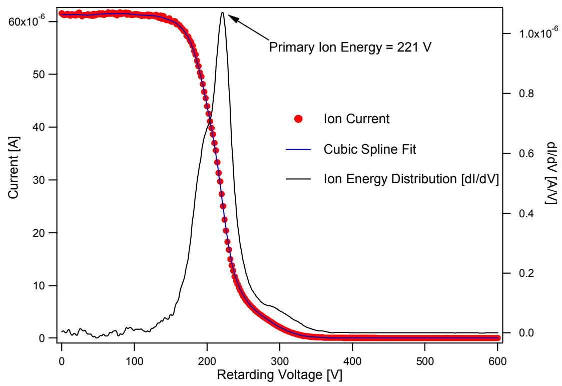

Figure 6: RPA current-voltage characteristic and ion energy distribution measured 5° off centerline.

Multiple traces were taken at each data point to verify the repeatability of RPA measurements. The repeatability was exceptional and is illustrated in Figure 7 by three traces taken at the same location as those of Figure 6.

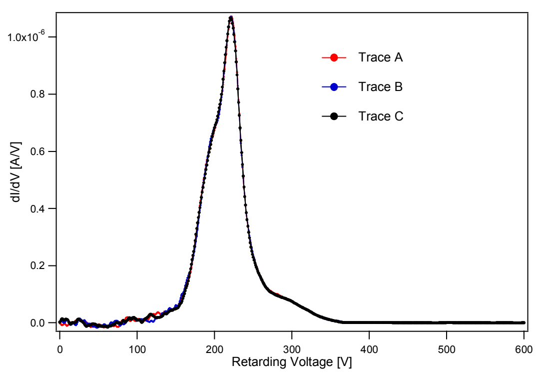

Figure 7: Multiple RPA traces illustrating the exceptional repeatability of the RPA diagnostic.

Experimental Configurations

The ESA and RPA were used to measure the ion energy distribution functions resulting from three different experimental configurations. In the first configuration, a single thruster was mounted in the chamber and the instruments were aligned to the thruster centerline. In the second configuration, the analyzers were aligned to the center point of the cluster and measurements were taken with all four thrusters operating. In the final arrangement, the instruments were aligned with the centerline of thruster 3. These arrangements are referred to throughout this paper as the single thruster, cluster, and offset cluster configurations, respectively. In each case, the instruments were mounted 0.5 m downstream of the thruster exit plane and the thrusters were rotated through an angular range of -90° to 90°. Data were collected at 5° increments between -30° and 30°, and at 10° increments over the remainder of the range. Figure 8 shows the ESA and RPA mounted in the chamber. The gridded and nude Faraday probes that can be seen to the right of the RPA in Figure 8 will be discussed in a future work.

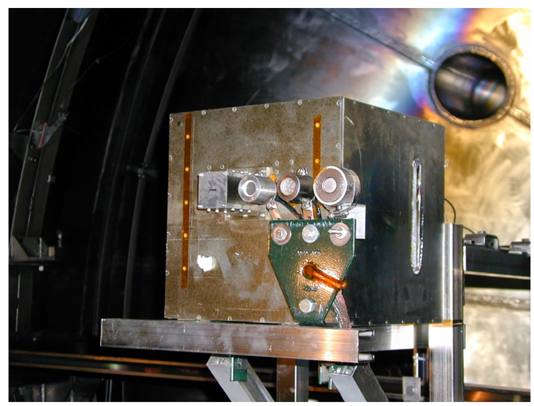

Figure 8: The energy analyzer and RPA installed in the LVTF.

Results and Discussion

Single Thruster

As an initial test of the diagnostics, energy distributions measured with the RPA were compared to those measured with the ESA for a single thruster. Figure 9 shows the measured distribution function for a single thruster at 0°, 15°, and 30° off centerline for each instrument. Notice the relatively good agreement between the two devices. For each of the three angular locations, the voltage at which the peak in the distribution function occurs agrees to within 8 volts. For example, on the thruster centerline the primary peak was measured at 220 volts by the RPA and at 228 volts by the ESA.

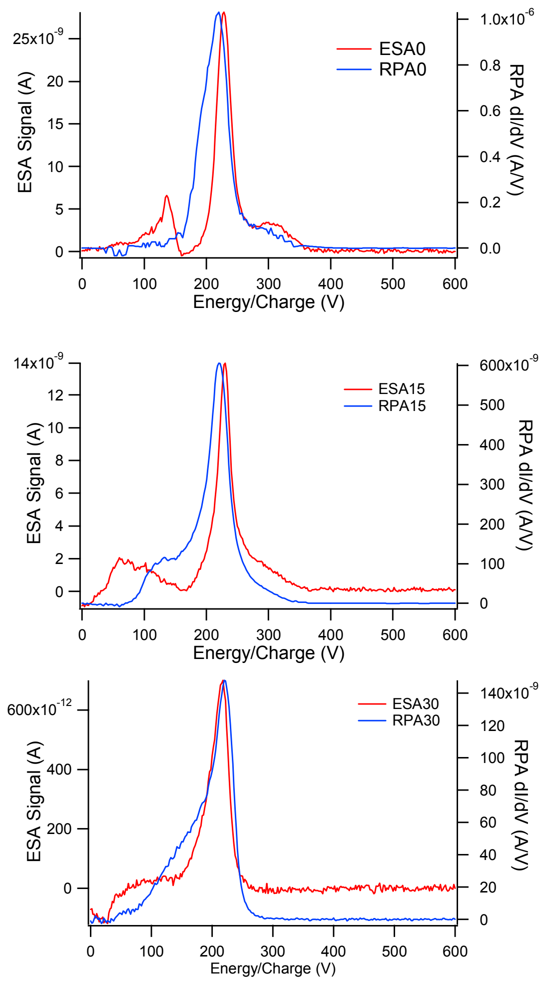

Figure 9: Ion energy distributions measured with the RPA and ESA at 0°, 15°, and 30° off centerline. Note the good agreement between the two diagnostics.

The most noticeable difference between the diagnostics demonstrated by Figure 9 is the appearance of secondary peaks at voltages above and below the primary ion voltage, which are more pronounced in the ESA traces. Additionally, the primary peak in the distribution is consistently wider when measured with the RPA as opposed to the ESA. The shape of the distribution function is likely to be more accurate in the ESA traces since those data are not subject to the smoothing effects of numerical differentiation. The location of the primary peak in the distribution, however, is likely to be more accurately depicted by the RPA because slight misalignment of the grid components would not be expected to alter the performance of this device. Slight misalignment or improper spacing of the plates in the ESA, on the other hand, could cause a shift of several volts in the measured distributions.

Figures 10 and 11 summarize the ion energy distributions recorded by the ESA, while Figures 12-14 depict similar data recorded by the RPA. Although traces were recorded for both positive and negative angles off centerline, only data for the positive angles are reported here due to the high degree of symmetry exhibited by the plume. The ESA traces show the peak ion energy to charge ratio to occur at approximately 228 volts for most of the angular spectrum, while the RPA shows the peak at 220 volts. The secondary structure occurring at energy to charge ratios below 150 volts can be attributed to elastically scattered primary ions.[9, 11] The high-energy population shown at voltages in excess of the discharge voltage, particularly at low angles off centerline, is likely due to beam ions that have undergone charge decreasing collisions.[6,9] Data are not shown for the ESA at angles greater than 60° due to the prohibitively small signal to noise ratio in this regime. RPA data, however, show the plume to be composed primarily of low energy charge exchange products at angles greater than 70°.

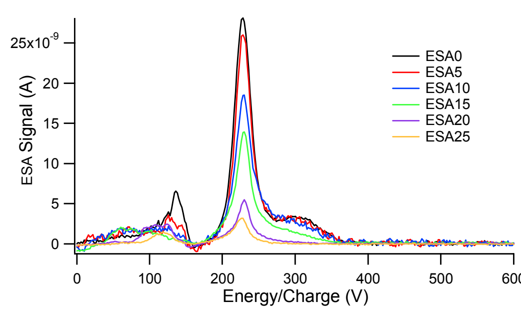

Figure 10: ESA data for a single thruster measured from 0°-25° off centerline.

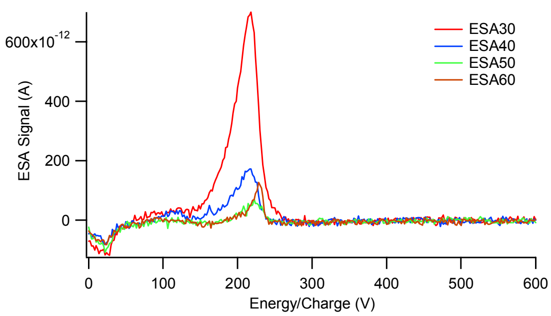

Figure 11: ESA data taken 30°-60° off centerline for a single thruster. Note the scale change from Figure 10.

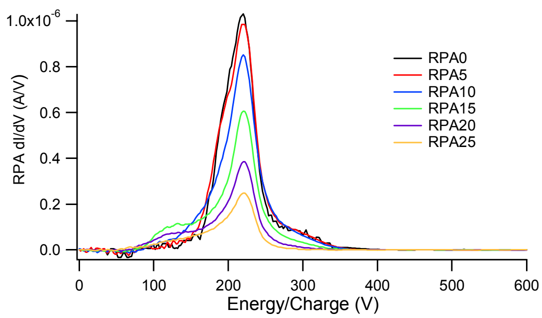

Figure 12: RPA traces taken 0°-25° off axis for a single thruster.

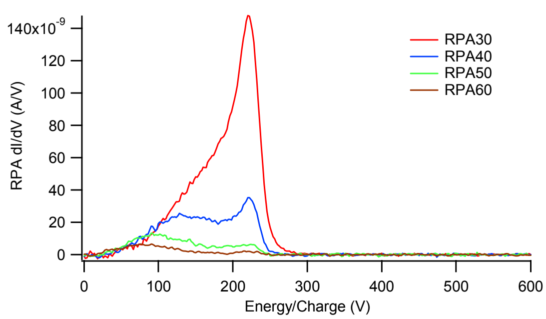

Figure 13: RPA data for a single thruster at angular positions of 30°-60°. Note the low energy tail due to elastic collisions.

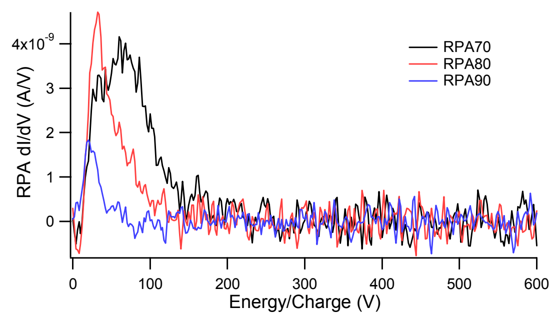

Figure 14: High angle, single thruster RPA data. At high angles, low energy charge exchange products dominate the spectrum.

Cluster

Unlike the data recorded for the single thruster case, the measurements obtained with the ESA and RPA aligned to the center of the cluster show marked differences between the two diagnostics. These differences are believed to be caused primarily by the different acceptance angles of the RPA and ESA. The ESA entrance slit provides an ion acceptance angle of approximately 4° in one direction and 0.5° in the other direction, while the cylindrical RPA has an acceptance cone half angle of approximately 25°. This discrepancy is not important for the case of a single thruster because both diagnostics are able to image the entire width of the thruster at a downstream distance of 0.5 m. At this distance, the ESA images a cross section only about 70 mm wide. In the cluster configuration, this results in the ESA imaging the space between the thrusters rather than the thrusters themselves. The RPA, on the other hand, has a wide enough viewing angle to accept ions originating from any of the four thrusters.

Figures 15 and 16 summarize the cluster data collected with the parallel plate energy analyzer. At angular positions less than 10° with respect to centerline, the peak in the distribution occurs at energy to charge ratios near the 250 volt discharge voltage. Between 10° and 20° the peak shifts down to approximately 134 volts, which is near the voltage of the elastically scattered ions measured in the plume of a single thruster. The 134 volt peak can be observed out to 80° off the cluster axis before the signal is lost between 80° and 90°. It should be noted that the signal level recorded by the ESA in this configuration is approximately a factor of 25 lower than that measured for a single thruster.

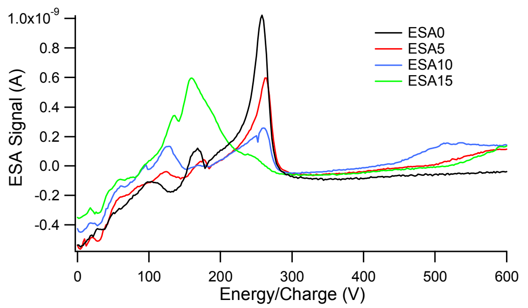

Figure 15: ESA traces at low angles off the cluster centerline. The instrument images the area between the thrusters.

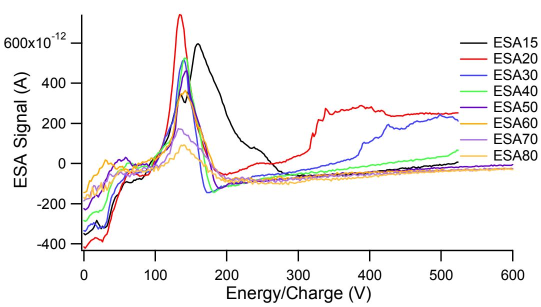

Figure 16: ESA traces at 15°-80° off the cluster centerline. Note the consistent peak location at approximately 134 volts.

The RPA data presented in Figures 17-19 show several unusual characteristics, particularly along the cluster centerline where the spectrum shows three distinct, repeatable peaks at 224, 116, and 74 volts. As explained by King, the peaks at 116 and 74 volts could be caused by ions exiting the thruster at a beam velocity, V_b, of 224 volts before undergoing charge exchange (CEX) collisions that result in populations with energy to charge ratios of approximately $V_b/2$ and $V_b/3$, respectively.[6] Just 5° off centerline, however, the spectrum changes to a double peaked structure with equally abundant populations occurring at 122 and 222 volts. As the angle off centerline is increased, the two peaks merge together to form a single peak near 206 volts with a low energy tail as shown in Figure 18. The fact that the ratio between the peak voltages changes as a function of angle seems to indicate that, if the multi-peak structure is due to collisions, the dominant interactions are likely elastic rather than CEX. However, the shift of the low energy population to higher voltage with increasing angle seen in Figure 17 is opposite to previously reported trends.[9] This suggests that a physical mechanism other than collisions may be responsible for this feature. At angles greater than 50° with respect to the thrust axis, the spectra are dominated by a low-energy population that shifts to lower voltages with increasing angles.

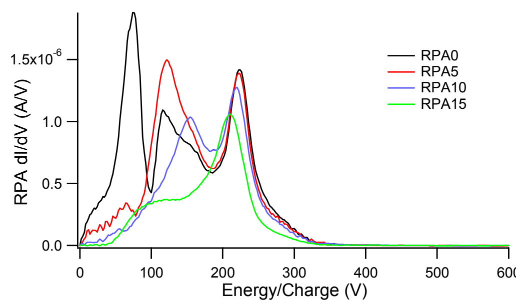

Figure 17: RPA data at angles less than 15° off the cluster centerline. Notice the distinct double peak at low angles.

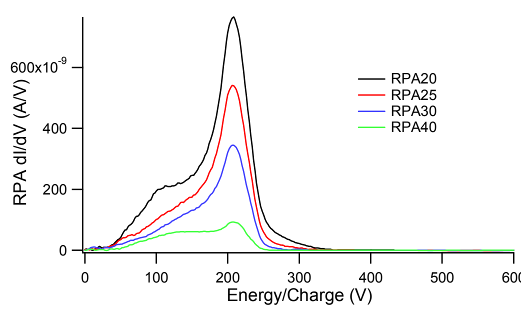

Figure 18: RPA traces taken at angles 20°-40° off the cluster centerline. Notice the low energy tail caused by elastic collisions.

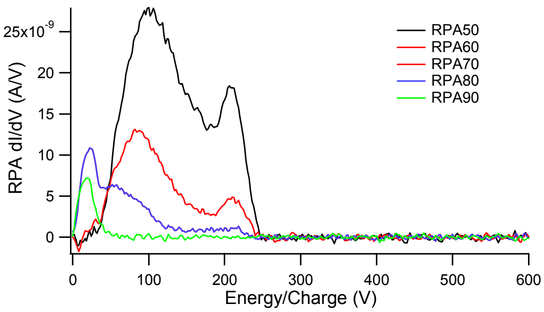

Figure 19: Energy per charge distributions measured 50°-90° off the cluster centerline. At high angles, low-energy charge exchange products dominate the spectrum.

In addition to collisions, a possible contributing factor to the low-energy structure involves ion focusing as a result of clustering. The plasma potential profile downstream of a cluster is fundamentally different than the profile in the plume of a single thruster. When ions exit a single Hall thruster, they experience a continuous decline in plasma potential regardless of the direction in which they exit the thruster. In other words, the electric field vector is everywhere directed away from the thruster. When multiple thrusters are operated together, however, this is not the case since a minimum in the plasma potential occurs in the region between the thrusters. This results in a situation where an ion directed toward the center of the cluster can be deflected downstream by the plasma potential "hill" created by adjacent thrusters. This situation is sketched in Figure 20 below, in which the blue lines represent contours of constant plasma potential and the red lines represent the paths of sample ions. The phenomenon illustrated in Figure 20 may lead to ion focusing in which ions initially directed toward the cluster center are deflected to lower angles with respect to the cluster centerline. This effect may be responsible for the slightly reduced beam divergence reported by Hargus *et al.* for two operating thrusters compared to that predicted by linear superposition of the ion flux from individual thrusters.[12]

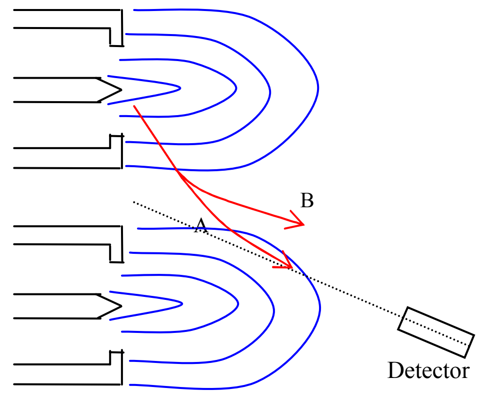

Figure 20: A qualitative sketch of the plasma potential profiles and altered ion trajectories induced as a result of clustering.

The mechanism of ion focusing presented here requires additional analysis before its effects on the plasma plume can be evaluated quantitatively. However, one can gain insight into several aspects of the energy spectrum by resorting to a simple phenomenological discussion. Consider two ions, A and B, exiting a thruster and traveling in an identical direction toward the center of the cluster, but with different initial kinetic energies. In this situation, the slower moving ion, B, would be deflected by a given potential rise to a greater degree than its high energy counterpart, ion A, as depicted in Figure 20. Considering this, a detector swept through the plume would detect ion A at a higher angle off centerline, while ion B with its lower energy would be deflected further downstream and detected at a relatively low angle. This phenomenon may account for the secondary structure shown in Figure 17, in which the low energy population shifts to higher voltages with increasing angle off centerline. This feature is only observable during cluster operation and is most pronounced at low angles.

Offset Cluster

For the offset cluster case, the ESA acceptance angle allows imaging of thruster 3, but none of the other three thrusters. As shown in Figures 21-23, the collected data appear qualitatively similar to the single thruster traces. The most striking difference is that the peak in the energy per charge distribution function has shifted to approximately 260 volts, which is 10 volts greater than the discharge voltage. At first glance, this peak shift appears to indicate a malfunction of the energy analyzer since there is no clear reason to expect the peak to occur at potentials greater than the discharge voltage. Further examination, however, shows that the secondary structure seen at low energies occurs at approximately 134 volts, just as it did for the single thruster and cluster cases. If the shift in the primary peak were caused by a malfunction of the instrument, one would expect the location of the secondary peak to shift also. Confidence in the instrument is further gained from the consistency of the data collection method. Data showing the primary peak at 225-230 volts were collected with a single thruster in operation immediately prior to the offset cluster measurements. The only difference between the two experimental procedures was the number of thrusters operating. The high voltage of the primary peak in the offset cluster data is therefore not fully understood.

An additional feature observable in Figures 22 and 23 is the predominance of the low-energy peak at angles above 40°. While this population can be seen in the single thruster traces at low angles, its magnitude is much less than that of the primary peak at angles greater than 30° off centerline. In the offset cluster data, the low-energy ions dominate the spectra from 40° to 80° and appear to indicate a drastic increase in the proportion of elastically scattered ions as a result of clustering.

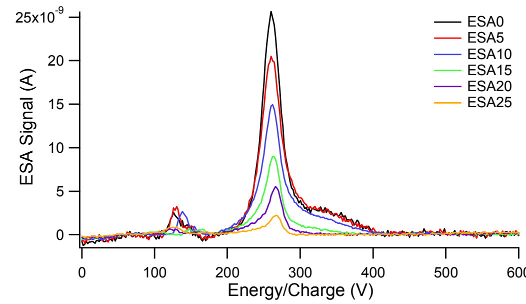

Figure 21: ESA traces 0°-25° off the centerline of thruster 3 with all four thrusters operating.

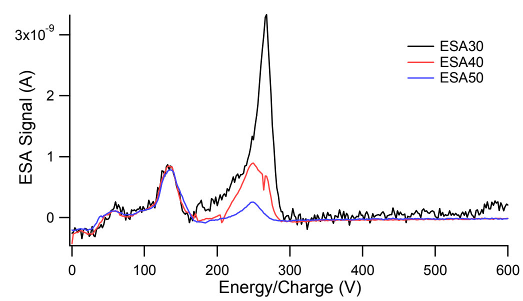

Figure 22: Energy distributions from 30°-50° off centerline in the offset cluster configuration. Note the constancy of the low energy peak at 134 volts.

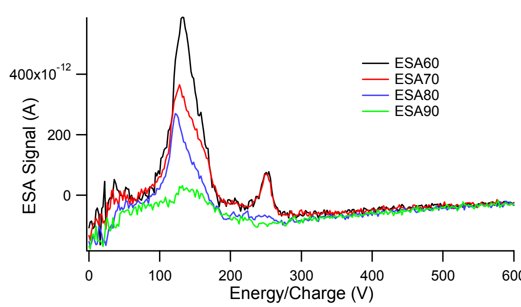

Figure 23: The ion energy distribution measured by the ESA at 60°-90°.

Figures 24-26 below show data taken with the RPA in the offset cluster configuration. Unlike the ESA, the RPA has a sufficiently wide viewing angle to accept ions from all four thrusters simultaneously in this configuration. The low angle traces show a primary peak at 226 volts and a wide secondary structure occurring between 100 and 170 volts. The absence of this structure in the single thruster data indicates that it is an effect of clustering multiple thrusters. Since the cluster spacing produces an angle of only 12.8° between the RPA normal and adjacent thrusters (TH 2 and TH 4), primary ions originating from these locations would be expected to be detected at energies within 5% of the 220-230 volt primary peak. The low energy structure therefore cannot be explained as simply a geometric effect due to primary ions entering the instrument at an incident angle. Rather, it is most likely a result of increased elastic scattering due to operating multiple thrusters. The ion focusing mechanism discussed previously may also play a role in the appearance of this feature during cluster operation. The relatively small magnitude of the corresponding low energy structure shown in Figure 21 supports the notion that the majority of the ions forming this feature originate at locations outside the ESA's field of view.

Similar to the trend shown in the ordinary cluster configuration, the primary peak in the offset cluster data gradually shifts to lower voltages at angles greater than 10° off centerline. This differs significantly from the single thruster case in which the primary peak remained detectable near 220 volts out to an angle of 50°. As shown in Figures 24 and 25, the peak shifts down to approximately 200 volts above 20°, and the low-energy ions begin to dominate the spectrum at angles greater than 60°.

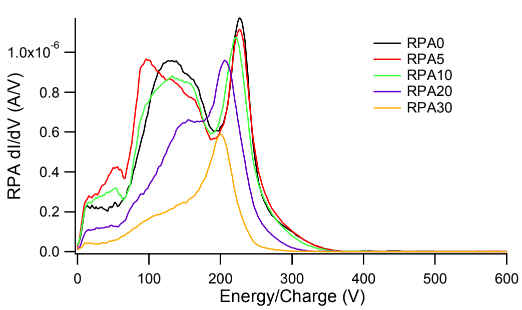

Figure 24: Low angle RPA data for the offset cluster configuration.

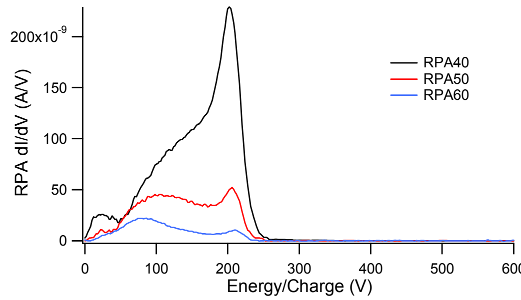

Figure 25: RPA traces taken 40°-60° off centerline of the offset cluster.

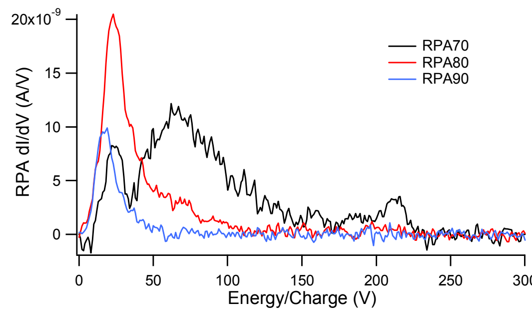

Figure 26: High angle RPA data for the offset cluster.

Conclusions

Two devices for measuring ion energy distributions, the electrostatic energy analyzer and the retarding potential analyzer, were tested in the plume of a low-power Hall thruster. Spectra obtained from these devices proved to be very repeatable and in good agreement with each other. Features seen in the plume compared favorably with previously published results.[6,8,9]

The ESA and RPA were then used to study the ion energy spectrum at various angular locations 0.5 meters downstream of a cluster of four low-power Hall thrusters. Data were collected both with the instruments aligned to the center of the cluster and with them aligned to the centerline of one of the four units. Compared to data obtained with a single thruster in operation, measurements taken for both cluster configurations indicate a profound increase in the fraction of low-energy ions, particularly at low angles off centerline. This feature is likely due to an increase in elastic scattering of primary ions as well as the unique plasma potential profiles expected downstream of a cluster.

Acknowledgements

The authors wish to express their gratitude to Dr. Mitat Birkan of the Air Force Office of Scientific Research for sponsoring this project and to Dr. William Hargus of the Air Force Research Laboratory for financial support and for the use of the cluster. We are especially grateful to Dr. James Haas of the Air Force Research Laboratory for his enormous contributions to this research. Dr. Haas designed and built the RPA discussed in this paper, as well as assisted in the performance of the experiments. This work was performed under the auspices of AFOSR Grant F49620-02-1-0051.

References

1. Spanjers, G.G., *et al*., "The USAF Electric Propulsion Research Program," AIAA-2000-3146, 36th Joint Propulsion Conference & Exhibit, Huntsville, AL, 2000.
2. Spores, R.A., *et al*., "Overview of the USAF Electric Propulsion Program," AIAA-2001-3225, 37th Joint Propulsion Conference & Exhibit, Salt Lake City, UT, 2001.
3. Hruby, V., *et al*., "Development of Low Power Hall Thrusters," AIAA-99-3534, 30th Plasmadynamics and Lasers Conference, Norfolk, VA 1999.
4. Hofer, R.R., *et al*., "Development of a 45-Degree Parallel-Plate Electrostatic Energy Analyzer for Hall Thruster Plume Studies: Preliminary Data," IEPC-99-113, 26th International Electric Propulsion Conference, Kitakyushu, Japan, 1999.
5. Pollard, J.E., "Plume Angular, Energy, and Mass Spectral Measurements with the T5 Ion Engine," 31st Joint Propulsion Conference & Exhibit, San Diego, CA, 1995.
6. King, L.B., Transport Property and Mass Spectral Measurements in the Plasma Exhaust Plume of a Hall-Effect Space Propulsion System, Ph.D Dissertation, University of Michigan, 1998.
7. Gulczinski III, F.S., *et al*., "Near-field Ion Energy and Species Measurements of a 5 kW Laboratory Hall Thruster," AIAA-99-2430, 35th Joint Propulsion Conference & Exhibit, Los Angeles, CA, 1999.
8. Gulczinski III, F.S., Examination of the Structure and Evolution of a 5 kW class Laboratory Hall Thruster at Various Operational Conditions, Ph.D Dissertation, University of Michigan, 1999.
9. Pollard, J.E., *et al*., "Ion Flux, Energy, and Charge-State Measurements for the BPT-4000 Hall Thruster," AIAA-2001-3351, 37th Joint Propulsion Conference & Exhibit, Salt Lake City, UT, 2001.
10. Hutchinson, I.H., Principles of Plasma Diagnostics, Cambridge University Press, 2002.
11. Katz, I., *et al*., "A Hall Effect Thruster Plume Model Including Large-Angle Elastic Scattering," AIAA-2001-3355, 37th Joint Propulsion Conference & Exhibit, Salt Lake City, UT, 2001.
12. Hargus, W.A. Jr., *et al*., "The Air Force Clustered Hall Thruster Program," AIAA-2002-3678, 38th Joint Propulsion Conference & Exhibit, Indianapolis, IN, 2002.